Progress In Electromagnetics Research C, Vol. 29, 97–107, 2012

CONICAL LINEAR SPIRAL ANTENNA FOR TRACKING, TELEMETRY AND COMMAND OF LOW EARTH ORBIT SATELLITES

K. F. A. Hussein*

Microwave Engineering Department, Electronics Research Institute (ERI), Dokki, Cairo, Egypt

Abstract—Conical log spiral antennas are famous for being appropriate for tracking, telemetry and command (TT&C) applications in low earth orbit (LEO) satellites. In this work, a conical linear (Archimedean) spiral antenna is introduced and investigated for the same purpose. The electric field integral equation (EFIE) technique is applied to a triangular-patch surface model of the conical equiangular linear spiral antenna. This antenna is optimized to produce the radiation characteristics required for TT&C applications for LEO satellites. The input impedance, polarization and radiation patterns of this antenna are investigated over the operating band of frequencies. Some of the obtained results especially those concerning the input impedance, radiation pattern, polarization and bandwidth are verified experimentally. It is shown that the proposed antenna is quite appropriate for TT&C in LEO satellite applications.

1. INTRODUCTION

Wide band broad beam circularly polarized antennas [1] are commonly required for LEO satellite applications. The conical equiangular log spiral antenna with a large number of turns has its input impedance, gain and polarization independent of frequency over a wide frequency band [2, 3]. It finds various applications in satellite communications, radar and electromagnetic compatibility [4]. Also, the conical equiangular log spiral satisfies the desired criteria of high performance satellite antennas such as GPS, telemetry and command antennas [5].

Received 16 March 2012, Accepted 28 April 2012, Scheduled 10 May 2012

* Corresponding author: Khalid Fawzy Ahmed Hussein (Khalid_elgabaly@yahoo.com).

Up to the author's knowledge, the conical linear spiral antenna was investigated only in [6] for a similar purpose. The present work introduces a two-arm conical linear spiral antenna with relatively small number of turns, small height and light weight. The antenna performance regarding the input impedance, polarization and radiation patterns for the circularly polarized components of the radiated field, is investigated over the operating frequency band.

The EFIE technique, described by Rao-Wilton-Glisson [7, 8], is applied to deal with the conical equiangular linear spiral structure using triangular patches to model the antenna surface. As the antenna is constructed up as conducting surface, the EFIE technique is the most appropriate method to deal with such an antenna. An integral equation is formulated for the unknown current distribution on the antenna surface. The integral equation is then converted to a linear system of equations, which can be solved using numerical techniques. Once the current distribution on the antenna surface is obtained, the far field, near field and the antenna input impedance can be directly calculated with a little numerical effort. The main numerical effort involved in the EFIE technique is only the solution of the linear system of equations, which is a simple computational task if compared with the computational requirements of other computational techniques, like the FDTD method, when used to treat the same antenna. Moreover, the geometrical model of the antenna used in the present work is very accurate and is almost identical to the actual surface of the antenna even when using a relatively small number of triangular patches.

The antenna performance is investigated numerically through computer simulation and experimentally by using a simply manufactured prototype for the proposed antenna. Both numerical and experimental results are presented and discussed.

2. ANTENNA GEOMETRY AND MODELING

The geometry of the conical equiangular linear spiral is described by the base diameter D, diameter of the truncated section at the vertex of the cone d, half-cone angle θ_o, wrapping angle α and arm angular width δ. We can add to these geometrical parameters the ending angle of the spiral arm ϕ_e, which is not an independent parameter and can be calculated from the other parameters.

As shown in Figure 1(a), each arm of the conical linear spiral antenna has two boundary curves. Let r_{s_1}, r_{e_1} be the boundary curves of the first spiral arm and r_{s_2}, r_{e_2} be those of the second arm. Each of r_{s_1}, r_{e_1}, r_{s_2} and r_{e_2} describes the distance from the apex of the cone to a point on one of the boundary curves of each arm. Thus, they can

be expressed as follows.

$$r_{s_1}(\phi) = r_o + a\,|\phi|\,, \quad |\phi| \geq 0 \tag{1}$$
$$r_{e_1}(\phi) = r_o + a(|\phi| - \delta), \quad |\phi| \geq \delta \tag{2}$$

$$r_{s_2}(\phi) = r_o + a(|\phi| - \pi), \quad |\phi| \geq \pi \tag{3}$$
$$r_{e_2}(\phi) = r_o + a(|\phi| - \pi - \delta), \quad |\phi| \geq \pi + \delta \tag{4}$$

where a is the spiral constant

The surface of the antenna can be modeled by triangular patches as shown in Figure 1(c). This method of modeling is simple and is suitable for accurate representation of curved surfaces provided that the number of patches is large enough. Also, it gives the possibility of varying the density of the triangular patches (number of patches per unit area of the surface) so that it becomes higher for the curved parts of the surface and lower for the straight parts. This enables accurate modeling of the antenna surface with the minimum number of patches.

Each of the triangular patches constituting the surface of the conical spiral antenna has three edges. An edge that belongs to only one triangular patch is a boundary edge and the electric current normal to it must be zero. An edge that is shared between two adjacent patches is a non-boundary edge and can have a current component flowing normal to it. Two adjacent triangular patches P_{n^+} and P_{n^-} sharing the edge number n are shown in Figure 2. A point in P_{n^+} can be specified by the position vector $\mathbf{r}_{n^+}$ defined with respect to the origin O, or by the position vector $\boldsymbol{\rho}_{n^+}$ defined with respect to the free vertex of the triangular facet P_{n^+} (i.e., the vertex of P_{n^+} which

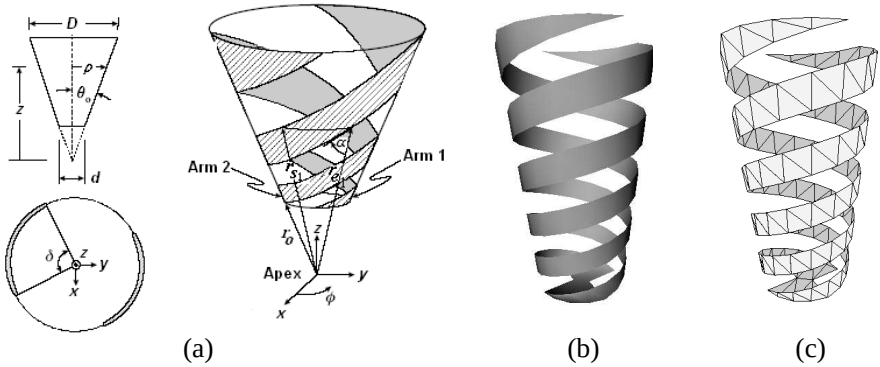

Figure 1. Geometric model of the conical spiral antenna. (a) Geometrical parameters. (b) Actual surface. (c) Triangular patch model.

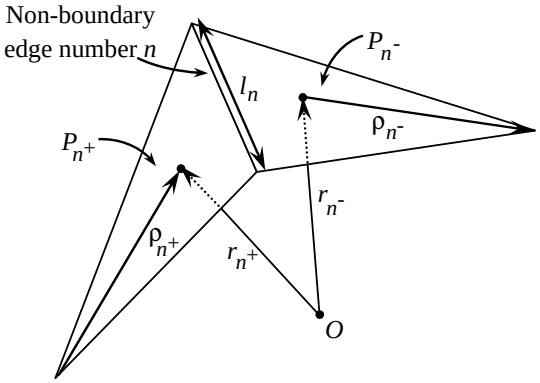

Figure 2. Two triangular patches sharing an edge.

does not belong to P_{n^-}). Similarly, a point in P_{n^-} can be specified by $\mathbf{r}_{n^-}$ or $\boldsymbol{\rho}_{n^-}$. It should be noticed that the position vector $\boldsymbol{\rho}_{n^+}$ is directed from the free vertex of P_{n^+} toward the point in the patch whereas the position vector $\boldsymbol{\rho}_{n^-}$ is directed from the point to the free vertex of P_{n^-}. The plus or minus designation of the triangular patches is determined by the choice of a positive current reference direction for the non-boundary edge number n, which is assumed to be from P_{n^+} to P_{n^-}.

3. ANALYSIS AND DESIGN

Consider that the antenna is excited by a gap generator (of unit voltage) and cut along one of the non-boundary edges of the antenna geometric model described above as shown in Figure 3. This means that upon crossing this edge, a voltage drop of one Volt is encountered. It should be noted that except for the edge of excitation, the voltage drop is encountered when crossing any other edge is zero. Thus, the voltage vector in the matrix equation, resulting from applying the moment method, has unity at the location corresponding to the edge of excitation and zeros elsewhere.

Let N_L be the number of one of the non-boundary edges taken at regular angular intervals along the spiral arm and indicated by the normal arrows as shown in Figure 4. According to the above considerations, the current distribution along the spiral arm length is represented by the values of I_{N_L}, which are the coefficients of the basis functions defined on the non-boundary edges, each of which can be numbered as N_L. The current at the feeding point is determined

by the value of I_{N_C}, which is the value of the coefficient of the basis function defined at the central edge, and where N_C is the number of that edge. This coefficient has a special importance as it represents the current at the antenna input port and, since the applied voltage is unity, the input impedance of the antenna is, simply, $1/(l_{N_C}^2 I_{N_C})$, where l_{N_C} is the length of the non-boundary edge at the excitation.

The conical spiral antenna shown in Figure 5 is proposed in the

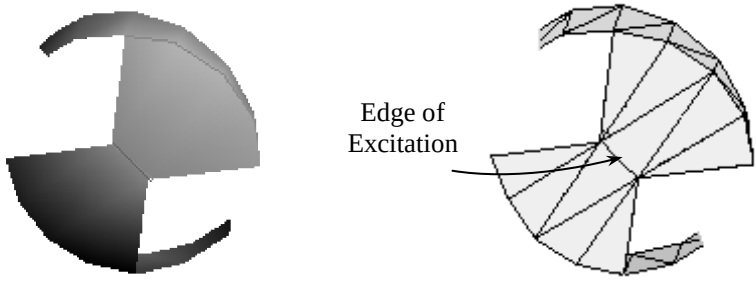

Figure 3. Gap voltage generator cut along one of the non-boundary edges of the antenna triangular patch model. (a) Antenna bottom where the exciting voltage is applied. (b) Triangular patches at the excitation.

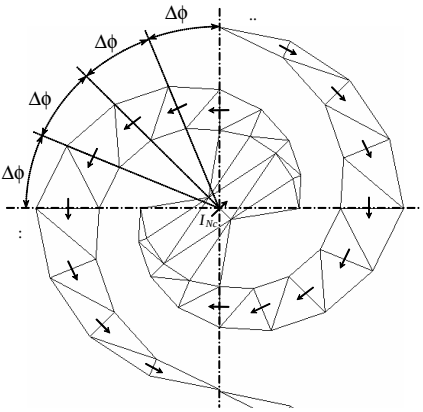

Figure 4. Direction of the current along the spiral arms which are divided into equal angular intervals.

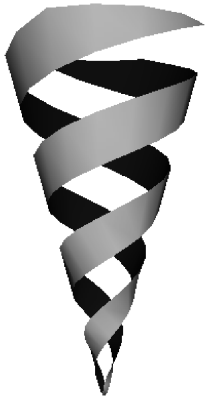

Figure 5. Shape of the proposed conical spiral linear antenna.

present work to give the desired conical shaped radiation pattern for uniform coverage when mounted on a LEO satellite. This antenna, when operates at 2.0 GHz, has the following geometrical parameters: $a = 13.17\,\text{mm/rad.}$, $\theta_o = 15°$, $d = 3.0\,\text{mm}$, $r_o = 5.8\,\text{mm}$, $D = 88.65\,\text{mm}$, and antenna height $= 159.8\,\text{mm}$.

4. NUMERICAL RESULTS AND DISCUSSION

A Microsoft Visual C++® program has been developed to generate a model for the conical spiral antenna and to apply the EFIE technique to calculate the current, input impedance and radiation patterns. The elevation and azimuth radiation patterns are shown in Figures 6 and 7, respectively. It is shown that the elevation radiation patterns represent conical beam where the radiation field at nadir is reduced to about 5 dB of its maximum value which occurs at about 65° with nadir. The azimuth pattern indicates omnidirectional radiation, which meets the requirements from such an antenna.

Figure 8 shows the variation of the input impedance of the antenna in the frequency band (1.9–2.1 GHz). The input impedance is almost stable and pure resistive over the operating frequency band.

Figures 9(a) and 9(b) show the patterns of the circularly polarized components and the axial ratio, respectively. It is clear that the axial ratio in the 0°-direction is about 7 dB, but however, is better in the other directions of interest.

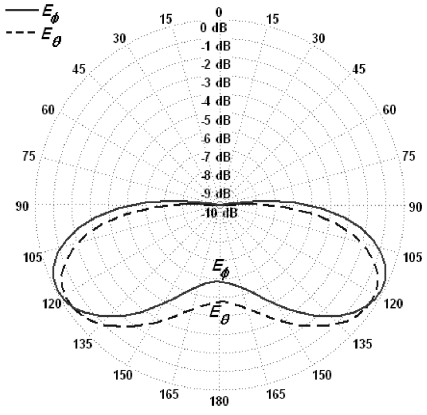

Figure 6. Elevation radiation patterns in the elevation plane $\phi = 0$.

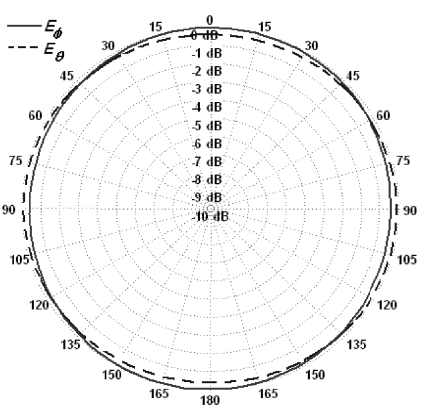

Figure 7. Azimuth radiation patterns; $\theta = 120°$.

5. ANTENNA CONSTRUCTION AND FEEDING

To construct a prototype for experimental testing of the antenna performance, the unwrapped cone and antenna arms are drawn on a sheet of paper as shown in Figure 10. The strips for the antenna arms are then cut on a metallic sheet as shown in Figure 11(a). The conical surface is constructed by wrapping a sheet of paper. The metallic strips are, then, wrapped on the cone.

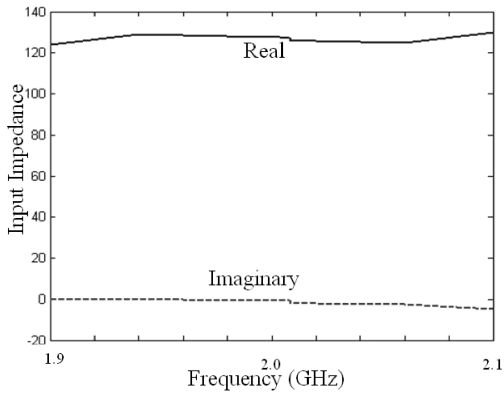

Figure 8. Input impedance.

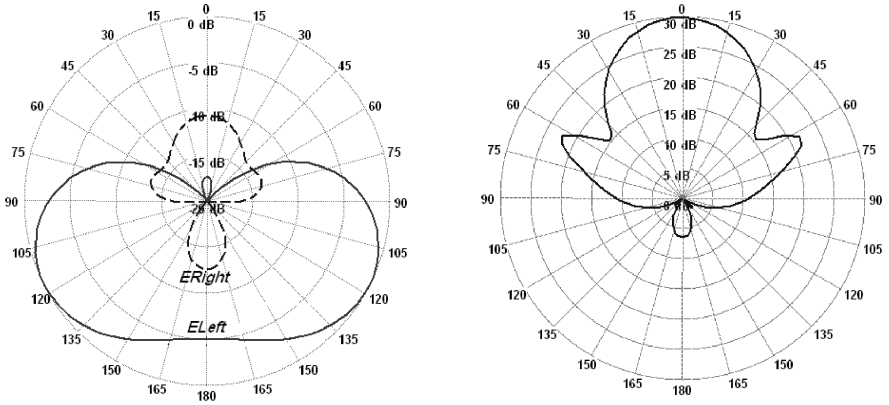

Figure 9. (a) Radiation patterns of the circularly polarized components (E-left and E-right) in the elevation plane $\phi = 0$. (b) Axial ratio pattern in the elevation plane $\phi = 0$.

Since the antenna should be fed by a balanced transmission line, a balun must be used. In the present case a balun (50 Ω BNC-120 Ω TWIN) is used for this purpose.

6. ANTENNA MEASUREMENTS

The input impedance of the conical spiral antenna and the directional patterns of the circularly polarized components of the radiation field are evaluated experimentally and compared to those obtained theoretically.

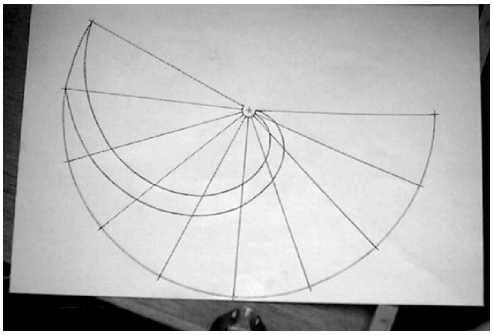

Figure 10. The edges of the spiral strip are drawn on the unwrapped surface of the cone on which the antenna strips are to be wrapped.

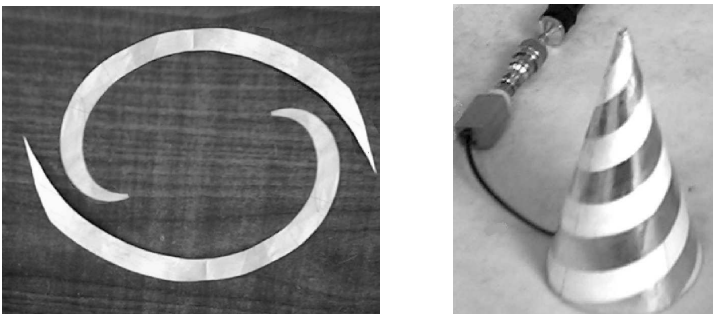

(a) (b)

Figure 11. Construction of conical spiral by wrapping the metallic strips on a cone made of paper. (a) Spiral strips are cut on a metallic sheet. (b) Spiral strips are wrapped on the cone.

6.1. Input Impedance Measurements

The vector network analyzer model Agilent-8719ES is used to measure the input impedance of the conical spiral antenna over the frequency range (1.9–2.0 GHz). The conical spiral antenna is connected to the analyzer as shown in Figure 12, where the input impedance is measured in the desired band of frequency. The experimental results of the input impedance measurements are presented in Figure 13. The experimental results show good agreement with those of computer simulation presented in Figure 8.

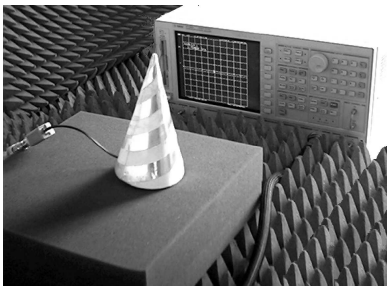

Figure 12. The Agilent network analyzer used for input impedance measurement.

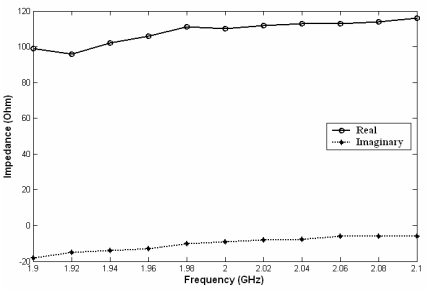

Figure 13. Measured input impedance of the conical spiral antenna.

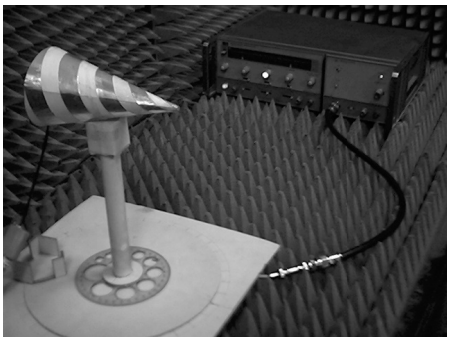

Figure 14. The microwave generator, the rotator and the radiation pattern measurement setup (not including receiving antenna, power sensor and power meter).

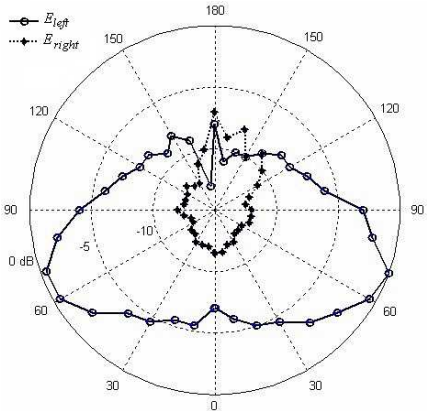

Figure 15. Measured radiation patterns for the left-hand and right-hand circularly polarized components radiated by the conical spiral antenna.

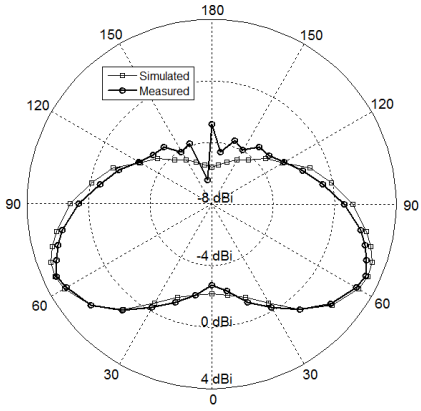

Figure 16. Comparison between simulated and measured gain patterns for the left-hand circularly polarized components radiated by the conical spiral antenna.

6.2. Radiation Pattern, Gain and Polarization Measurements

The experimental setup for radiation pattern measurements is shown in Figure 14. For measuring the left-hand and right-hand circularly polarized components of the field radiated from the conical spiral antenna, two helical antennas of opposite winding directions and almost circular polarization are used. The radiation patterns are measured and plotted as shown in Figure 15. A comparison between computer simulation and measurement results for the gain pattern of the left-hand circular polarization is presented in Figure 16. The experimental results can be considered in good agreement with the computational results obtained above, Figure 9(a).

7. CONCLUSION

A conical equiangular linear spiral antenna is optimized to produce the radiation characteristics required for TT&C in LEO satellite applications. The antenna is modeled using triangular-patch surface model. The EFIE technique is applied to analyze the antenna characteristics. The input impedance and radiation patterns of this antenna are investigated over the operating band of frequencies. The obtained results concerning the input impedance, radiation pattern, gain, polarization and bandwidth are verified experimentally.

REFERENCES

1. Sun, L., Y.-J. Sun, Y.-H. Huang, B.-H. Sun, and Q.-Z. Liu, "A novel wide band and broad beamwidth circularly polarized," *Journal of Electromagnetic Waves and Applications*, Vol. 25, No. 10, 1459–1470, 2011.
2. Hussein, K. F. A., "Analysis of conical equiangular spiral antenna using EFIE technique," *National Radio Science NRCS'2004*, Vol. 21, 1–11, Cairo, Egypt, March 2004.
3. Hertel, T. W. and G. S. Smith, "Analysis and design of two-arm conical spiral antennas," *IEEE Trans. Electromagn. Compat.*, Vol. 44, No. 1, 25–37, 2002.
4. Hertel, T. W. and G. S. Smith, "On the dispersive properties of the conical spiral antenna and its use for pulsed radiation," *IEEE Trans. Antennas Propagat.*, Vol. 51, No. 7, 1426–1433, 2003.
5. Padros, N., J. I. Ortigosa, J. Baker, and M. F. Iskander, "Comparative study of high-performance GPS receiving antenna designs," *IEEE Trans. Antennas Propagat.*, Vol. 45, No. 4, 698–706, 1997.
6. Zhu, Y. and J. Xu, "Design of two-arm conical spiral antenna for low elevation angle communication," *Journal of Electromagnetic Waves and Applications*, Vol. 24, Nos. 5–6, 785–794, 2010.
7. Rao, S. M., D. R. Wilton, and A. W. Glisson, "Electromagnetic scattering by surfaces of arbitrary shape," *IEEE Trans. Antennas Propagat.*, Vol. 30, No. 3, 409–418, 1982.
8. Hussein, K. F. A., "Fast computational algoritm for EFIE applied to arbitrarily-shaped conducting surfaces," *Progress In Electromagnetics Research*, Vol. 68, 339–357, 2007.